

Two-Dimensional Simulation of Fluid Instability in Laser-Fusion Pellets

J. D. Lindl and W. C. Mead

Lawrence Livermore Laboratory, University of California, Livermore, California 94550

(Received 9 December 1974)

Two-dimensional numerical-simulation techniques have been used to study fluid instability in laser-fusion pellets. Comparisons with analytic solutions in nonablating test cases show good agreement. Isentropic ablative accelerations exhibit growth rates 50%–100% of Rayleigh-Taylor values, while nonisentropic cases show suppressed growth. Design optimization has led to an impulsively accelerated, low-aspect-ratio shell which operates successfully with a surface perturbation of a few tens of angstroms.

If a DT sphere or shell is isentropically imploded by laser-driven ablation to a nearly Fermi degenerate, high-density state, inertially confined burn of the DT fuel can give high gain at laser energies below 100 kJ.¹ Attainment of this performance depends, among other factors, upon the behavior of Rayleigh-Taylor and convective instabilities at the ablating pellet surface. The most severe limitations of surface perturbations discussed here arise for wavelengths of the order of the minimum shell thickness. If these modes reach large amplitude, they result in a breakup of the shell and gross mixing of high- and low-density matter.

Recently, instability of the ablation surface has been studied using an analytic model and using numerical solutions of a linear perturbation approximation.² However, no consistent picture has yet emerged. Shiau, Goldman, and Weng present calculations of the adiabatic implosion of a DT sphere showing space-averaged growth rates for rms density perturbations at low mode numbers which are more than an order of magnitude greater than those for Rayleigh-Taylor modes. These averaged amplitudes cannot be directly compared with our amplitudes at the ablation surface which grow at the classical value for similar calculations. The calculations of Brueckner, Jorna, and Janda show the acceleration of a slab using a linearized code with a stationary zero-order solution. This limits the class of accelerations they can study and restricts the generality of their conclusions. The same difficulty arises in the work of Bodner² whose analytic model of the zero-order solution differs significantly from realistic laser-driven implosions.

The authors have utilized the computer code LASNEX^{1,3} to solve directly the full nonlinear, two-dimensional, fluid-dynamics equations. Using this axisymmetric Lagrangian finite-difference code, we have simulated fluid instability

and examined its significance for pellet design.⁴

The simulations utilize an integral number of half wavelengths bounded by a surface across which no matter flows for the normal mode to be studied. Surface perturbations were most frequently applied as a zig-zag surface deformation of four zones per wavelength, a technique discussed below. We then monitor space- and time-dependent amplitudes by computing rms deviations from the mean along the symmetry direction for the various material properties. Amplitude histories are obtained in cases with ablation by following the amplitudes near the peak-density surface. The validity of this technique has been verified by using LASNEX to compute perturbation growth rates for test problems having analytic solutions, over the parameter range given in Table I.

If an incompressible slab containing materials of density ρ' and ρ is accelerated in a direction perpendicular to the interface with acceleration a , then perturbations of the interface, having wave number $k = 2\pi/\lambda$, will grow as $\exp(\gamma t)$ with a rate

$$\gamma = (\alpha k a)^{1/2}, \quad (1)$$

TABLE I. Ranges of parameters covered by test problems: wave number k (cm^{-1}); mode number l ; acceleration a (10^{16} cm/sec^2); and growth rate γ (10^8 sec^{-1}). Results are summarized by giving average ratios of LASNEX to analytic growth rates for perturbations zoned with 4 (R_4) and 8 (R_8) zones per wavelength.

	Slab	Sphere
k	30–3000	...
l	...	50–600
a	0.05–500	0.5–50
γ	1–500	4–150
R_4	0.76 ± 0.03	0.80 ± 0.05
R_8	0.89 ± 0.03	0.92 ± 0.03

where $\alpha = (\rho' - \rho)/(\rho' + \rho)$ is the Atwood number. We chose test problems having $\alpha = 1$ for which $k\eta \ll 1$, to minimize effects of finite amplitude η ; $k\Delta R \gg 1$, to minimize effects of finite slab thickness; and $kc_s/\gamma \gg 1$ with c_s the sound speed, to minimize effects of compressibility. The average ratio of LASNEX growth rates to those predicted by Eq. (1) was 0.76 ± 0.03 .

A few slab examples having $\alpha = 0.5$ were run, and these showed correct reduction of growth rate. An $\alpha = -0.5$ case showed oscillatory, non-growing amplitudes, as expected.

Implosion and explosion of spherical shells by an external pressure source have been considered by Plessett.⁵ The average ratio of LASNEX growth rates to those predicted by Plessett is 0.80 ± 0.05 , with the use of 4 zones per wavelength.

The use of 4 zones per wavelength permits study of single modes, since wavelengths shorter than 4 zones are severely damped by the artificial viscosity in LASNEX. With higher transverse resolution, such as 16 zones per wavelength, very similar initial growth rates are obtained. But in regions of the dispersion relation where the growth rate is rapidly rising as the wavelength decreases, wavelengths shorter than the applied perturbation grow to dominant amplitudes from initial noise levels. Thus in a long implosion, mode shift eventually occurs to 4 zones per wavelength, unnecessarily complicating the analysis.

In our applications of LASNEX to low-adiabat implosions, we find no evidence for ablative stabilization. A comparison with the results of Henderson, McCrory, and Morse² for a reportedly stable solid-pellet implosion was thus of considerable interest. We have observed stable performance of their example for $l=5$ and $l=100$ spherical harmonic modes. For $l=5$, LASNEX amplitudes are in qualitative agreement and within a factor of 3 of quantitative agreement with the previous work.

To study the transition from unstable to stable implosions, we considered a solid DT sphere of radius $450 \mu\text{m}$ and density 0.21 g/cm^3 irradiated by a $1.06\text{-}\mu\text{m}$ -wavelength laser. Figure 1(a) shows a pulse (D) which is optimized for one-dimensional (1D) yield, neglecting multigroup transport effects. In Fig. 1(b) the implosion adiabats are shown for this pulse and for the chopped pulses C, B, and A. Also shown as dashed curves in the figure are the pulse shape and our calculation of the adiabat of the example of Henderson, Mc-

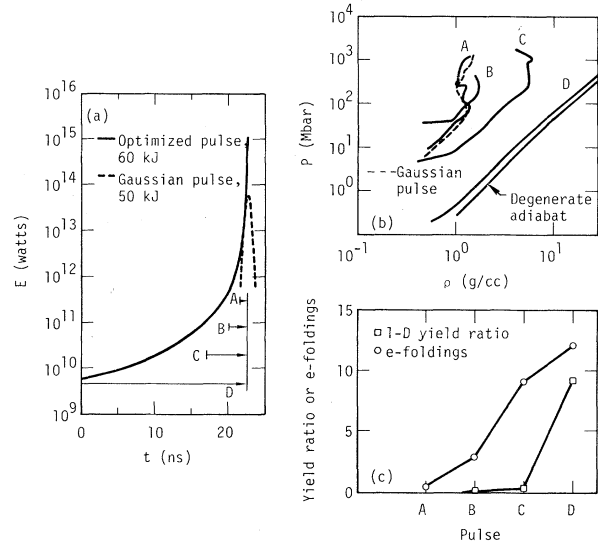


FIG. 1. Stability-yield examples: (a) Pulse shapes; (b) implosion adiabats; (c) 1D energy yield ratios and 2D calculated e foldings.

Crory, and Morse. The 1D yield ratios are shown in Fig. 1(c), clearly showing the importance of achieving a low adiabat.

When these pulse shapes are applied to a 2D slice of the pellet with a surface perturbation, the calculated number of e foldings varies as shown in Fig. 1(c). The most highly chopped pulse (A) is essentially stable, but as the implosion becomes more nearly isentropic growth increases until, for the full pulse (D), the instability reaches amplitudes which lead to failure of this design.

Other examples support this observation. Significant growth suppression is seen only in cases in which a shock of increasing strength propagates through cooler, less-dense material. Hence these stabilized implosions are nonisentropic and are energetically unsuitable for laser-fusion applications. In low-adiabat compressions, instability growth rates are insignificantly damped, and in fact are calculated to be in the range of 50% to 100% of classical Rayleigh-Taylor growth rates for wavelengths of interest.

We have concentrated design efforts on shells of DT ice with aspect ratios, $R/\Delta R$, from 1 to 60 with a 1D gain of between 20 and 60 and input energy of about 100 kJ. Shells with aspect ratios greater than 1 are of interest because they allow a reduction in the required laser power by increasing the volume of the target.¹

A model velocity history which shows the fac-

tors to be optimized to reduce Rayleigh-Taylor growth is the following: Assume the velocity increases linearly from zero to a fraction ϵ of the final velocity in a fraction $1 - \epsilon$ of the total implosion time, and then increases linearly to the final velocity in the remaining fraction ϵ of the time. Then the number of e foldings of growth for $k = 2\pi/\Delta R_{\min}$ is given by $n = [8\pi(1 - \epsilon)R_0/\Delta R_{\min}]^{1/2}$, where R_0 is the distance moved by the target. This equation ignores compression, which decreases the amplitude, and spherical convergence, which causes shifts to shorter wavelenths. To avoid shell breakup, the perturbation amplitude must remain less than the minimum shell thickness. This sets an upper limit, $N_{\max} \sim \ln(\Delta R_{\min}/\eta_0)$, for the tolerable number of generations of growth. This model shows that to survive instability, a design should minimize $R_0/\Delta R_{\min}$, maximize ϵ , or accelerate the shell as early in the implosion as possible, and minimize η_0 , the initial surface perturbation.

Figure 2 shows the implosion of a shell with an $R/\Delta R$ of 30 optimized for fluid instability. With an initial perturbation of 7 \AA rms, $l=160$ was the shortest wavelength that could be successfully imploded, as shown in Fig. 2(c). Compression and ablation greatly reduce the shell thickness during the implosion, allowing short, fast-growing wavelengths to destroy the shell. In Fig. 2(d), the isodensity contours for an $l=320$ perturbation show a typical failure mode.

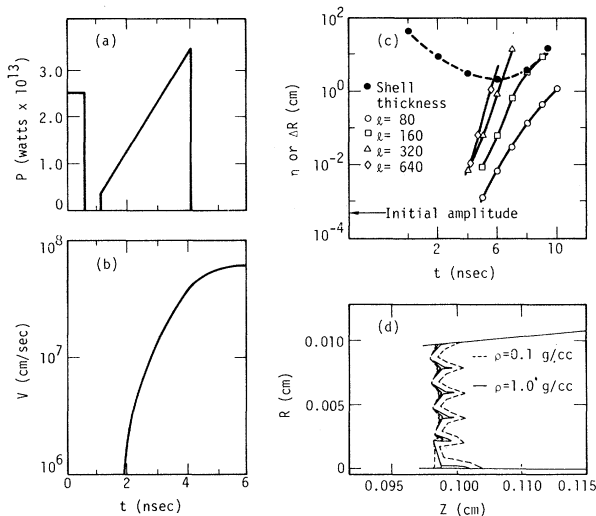


FIG. 2. Shell with $R/\Delta R$ of 30. (a) Pulse shape; (b) velocity history; (c) amplitude and shell-thickness histories; (d) isodensity plot of failure mode for $l=320$ at time 4.3 nsec.

To get an implosion which was successful with a realizable level of surface perturbation, we had to use targets with small aspect ratios and change from uniform acceleration to a series of chopped pulses which give an impulsive acceleration. From Eq. (1) it is evident that for a given velocity change, the number of generations of growth is inversely proportional to the square root of the acceleration. In the limit of a shock wave of zero thickness, growth is no longer exponential in time but linear, resulting from focusing as the shock passes a perturbed interface. The formula for this growth has been given by Richtmyer⁶ as $\dot{\eta} = \alpha k \Delta v \eta_0$, where $\dot{\eta}$ is the rate of change of the amplitude, and Δv is the difference in material velocity between the front and back of the shock. The smallest growth factor is obtained if a shell receives its entire velocity from a single shock. The growth factor increases as more shocks are used and approaches the Rayleigh-Taylor value in the limit of many small shocks. If the ratio of the amplitude of successive shocks is kept within about a factor of 4, and they are timed to prevent excessive decompression of the shell between shocks, the adiabat remains within an order of magnitude of the degenerate case. Shown in Fig. 3(a) is the laser power profile of a $\frac{1}{4}$ - μm laser applied to a 256- μg DT shell with outer radius of 700 μm and inner radius of 400 μm . The velocity shown in Fig. 3(b) is at the ablation surface where each successive shock is generated. The velocity there decreases as the pressure relaxes after each shock passes. Figure 3(c) shows the perturbation amplitude at the

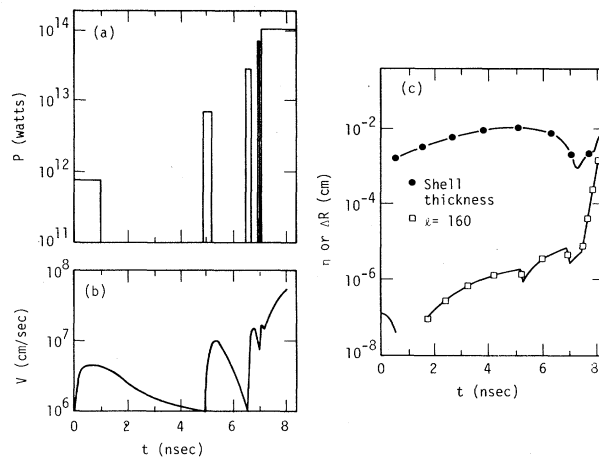


FIG. 3. Shell with $R/\Delta R$ of 2. (a) Pulse shape; (b) velocity history; (c) amplitude and shell-thickness history.

ablation surface and the shell thickness as a function of time for the worst unstable wavelength, $l=160$, for an initial amplitude of 14 \AA rms. After passage of the first shock, the linear growth in time of the perturbation is evident. We have examined the $l=320$ mode and the growth rate and final amplitude were little changed. The suppression of growth rate seen here at short wavelengths is consistent with expectations for instability with a finite density gradient.⁷

Since the dispersion relation is flat around $l=160$ for this implosion, we have been able to run the $l=160$ mode throughout the implosion with 8 zones per wavelength. We find less than a factor of 2 change in calculated final amplitudes. In this implosion, no appreciable degradation of the thermonuclear yield is caused by fluid instability, either during ablative acceleration or in deceleration prior to burn, for an initial amplitude of 14 \AA rms in the $l=160$ mode.

In a few test cases, we found that the effect of self-generated magnetic fields was negligible for surface-perturbed targets by use of the classical transport coefficients of Braginskii⁸ or Bohm diffusion. However, since the fields reduce thermal conduction, they can significantly increase the surface perturbations imprinted by a given illumination nonuniformity. Techniques for cre-

ating a low-density corona to minimize effects of nonuniform illumination are under study.

We find no significant change in the fluid instability behavior when multigroup electron transport is included in the calculation.

The authors would like to thank John Nuckolls for his comments, suggestions, and encouragement throughout this research, and George Zimmerman for the use of his code.

¹J. Nuckolls, L. Wood, A. Thiessen, and G. Zimmerman, *Nature* (London) **239**, 139 (1972).

²J. N. Shiao, E. B. Goldman, and C. I. Weng, *Phys. Rev. Lett.* **32**, 352 (1974); D. B. Henderson, R. L. McCrory, and R. L. Morse, *Phys. Rev. Lett.* **33**, 205 (1974); K. A. Brueckner, S. Jorna, and R. Janda, *Phys. Fluids* **17**, 1554 (1974); S. E. Bodner, *Phys. Rev. Lett.* **33**, 761 (1974).

³G. B. Zimmerman, University of California Report No. UCRL-74811, 1973 (unpublished).

⁴J. D. Lindl and W. C. Mead, University of California Reports No. UCRL-75877 and No. UCRL-75879, 1974 (unpublished).

⁵M. S. Plessett, *J. Appl. Phys.* **25**, 96 (1954).

⁶R. D. Richtmyer, *Commun. Pure Appl. Math.* **13**, 297 (1960).

⁷S. Chandrasekhar, *Hydrodynamic and Hydromagnetic Stability* (Oxford Univ. Press, London, 1968), p. 435.

⁸S. I. Braginskii, *Rev. Plasma Phys.* **1**, 205 (1965).

Knight Shift in Expanded Liquid Mercury

U. El-Hanany* and W. W. Warren, Jr.†

Bell Laboratories, Murray Hill, New Jersey 07974

(Received 13 March 1975)

We report the first magnetic data for an expanded liquid metal: the Knight shift in liquid Hg from the normal liquid density to less than 8 g/cm^3 at 1730 K and 1411 bar. An abrupt metal-nonmetal transition between 9 and 8 g/cm^3 is preceded by ranges of roughly linearly decreasing shift ($11 \lesssim \rho \lesssim 13.6 \text{ g/cm}^3$) and constant shift ($9 \lesssim \rho \lesssim 11 \text{ g/cm}^3$). The latter behavior fails to support current theories developed to explain electronic transport properties.

A simple band model of divalent metals predicts that if the density of atoms is reduced sufficiently, transformation to an insulating state should occur. The transformation results from narrowing and separation of the bands associated with the highest occupied atomic level and the first excited state. Because of its relatively low critical temperature and pressure, liquid Hg can be expanded to very low density by heating under pressure ($T_c = 1760 \text{ K}$, $P_c = 1510 \text{ bar}$). In this way

Franck and Hensel first observed a continuous metal-nonmetal transition in the dc electrical conductivity of expanded fluid Hg.¹ Their work and subsequent investigations of the conductivity,^{2,3} thermopower,^{2,3} and Hall coefficient⁴ show that Hg reaches a state of characteristically semiconducting behavior in the subcritical liquid at a density roughly 60% of that of the normal (room-temperature) liquid.

It has been generally supposed that splitting of